Journal of Mathematical Psychology 62–63 (2014) 22–32

Contents lists available at ScienceDirect

Journal of Mathematical Psychology

journal homepage: www.elsevier.com/locate/jmp

Piéron's Law is not just an artifact of the response mechanism

Chris Donkin [a,*], Leendert Van Maanen [b]

[a] School of Psychology, University of New South Wales, Australia

[b] Cognitive Science Center Amsterdam and Department of Psychology, University of Amsterdam, The Netherlands

HIGHLIGHTS

- Mean RT and stimulus strength are often related by a power law.
- Historically, this has been thought to reflect scaling of stimulus strength.
- Proposed that it may be a result of the architecture of the decision-making process.
- We show that at least sometimes the power law is a result of scaling, and not just decision-making.

ARTICLE INFO

Article history:
Received 8 August 2014

Keywords:
Piéron's Law
Response time
Evidence accumulation models
Sequential sampling models

ABSTRACT

Piéron's Law, the power relation between mean RT and stimulus intensity or discriminability, has historically been understood to reflect a non-linear scaling between objective intensity and perception. More recently, Piéron's Law was demonstrated to arise out of the architecture of rise-to-threshold decision-making models (Stafford and Gurney, 2004). Here we explicitly tested whether such an explanation would suffice to fit human data, or whether additional assumptions about the nature of perceptual processing are required. We fitted a simple rise-to-threshold model to full RT distributions and choice probabilities from three data sets that show Piéron's Law. The model assumed that accumulation rate was linearly related to perceptual processing, leaving only the architecture of the model to produce Piéron's Law. For two data sets, this linear rate model is unable to account for the data, suggesting that Piéron's Law sometimes reflects additional perceptual scaling information. For the third data set, however, Piéron's Law does appear to simply arise out of the rise-to-threshold architecture of decision-making models. Our results suggest that it is important to fit models to data in order to draw inference about the causes underlying Piéron's Law.

1. Introduction

Piéron's Law (Luce, 1986; Piéron, 1952) refers to the long established empirical regularity that the mean time taken to respond to a stimulus is a power function of its physical intensity, such that mean response time (RT) is

$$RT = R_0 + kI^{-\beta}$$

where R_0 is an intercept parameter, k and β are scaling parameters, and I is stimulus intensity.

Piéron (1914) originally proposed the law to account for the relationship between intensity (or luminance) and the average time taken to detect an item, though it has been extended to other forms of detection (e.g., odor, Overbosch, de Wijk, de Jonge, & Koester, 1989; taste, Bonnet, Zamora, Buratti, & Guirao, 1999; motion, Burr, Fiorentini, & Morrone, 1998; the influence of glare, Aguirre, Colombo, & Barraza, 2008). Piéron's Law has also been observed beyond simple detection. For example, Pins and Bonnet (1996) showed that Piéron's Law persists when stimulus intensity is manipulated in two-choice tasks. Stafford, Ingram, and Gurney (2011) demonstrated the law's persistence as a function of color saturation in a Stroop task (see also Servant, Montagnini, & Burle, 2014). Palmer, Huk, and Shadlen (2005) showed that a power-law relationship exists between mean RT and the coherence of moving dots in a random-dot kinematogram (see also Reddi, Asrress, & Carpenter, 2003), and Van Maanen, Grasman, Forstmann, and Wagenmakers (2012), also found Piéron's Law when manipulating the discriminability between response options in a moving dots task.

Piéron's Law has historically been considered as a theory of stimulus scaling, capturing the relationship between physical

* Correspondence to: School of Psychology, University of New South Wales, Kensington, NSW, 2052, Australia.
E-mail addresses: christopher.donkin@gmail.com (C. Donkin), l.vanmaanen@uva.nl (L. Van Maanen).

http://dx.doi.org/10.1016/j.jmp.2014.09.006
0022-2496/

changes in stimulus strength and psychological discriminability (Nachmias & Kocher, 1970). However, the commonality of Piéron's Law across so many paradigms has lead researchers (e.g., Stafford & Gurney, 2004; Van Maanen et al., 2012) to propose that Piéron's Law is unrelated to stimulus scaling, but is a result of the architecture of the response selection (or decision making) process.

Stafford and Gurney (2004) demonstrated that Piéron's Law naturally arose out of rise-to-threshold accumulation models of decision making (e.g. Ratcliff's Diffusion model, Ratcliff, 1978). They showed that as the intensity of a stimulus increased linearly, the increase in the average time taken to respond followed a power function. In addition, Van Maanen et al. (2012) showed that Piéron's Law also occurs in Bayesian ideal observer models of evidence accumulation in detection and two-alternative forced choice tasks. In particular, they showed that as the difficulty of a motion discrimination task increases (by reducing the angular distance between the directions of motion being discriminated), the ideal observer model predicts that mean RTs will follow a power function. Importantly, both sets of authors (Van Maanen et al., and Stafford & Gurney, 2004) showed that Piéron's Law held across a range of parameter values, and was due to the architecture of the decision making process rather than specific parameter settings in the models.

That Piéron's Law could be a simple artifact of the response selection mechanism is an attractive prospect. For one, Piéron's Law arises elegantly and naturally from the rise-to-threshold architecture of decision-making models. Further, the models were not developed to account for this regularity. However, the question remains as to whether the response mechanism is solely responsible for Piéron's Law, or if the scaling of stimulus strength is also underlying the empirical observation of Piéron's Law.

Our aim in this paper is to provide a strict test of whether it is possible to use only on the architecture of a response selection mechanism to account for empirical data that shows Piéron's Law. We will use a simple version of the Linear Ballistic Accumulator (LBA, Brown & Heathcote, 2008) to test whether the architecture of the model alone can fit a number of benchmark data sets. We begin with a brief introduction to the LBA model, and show that Piéron's Law falls from the architecture of the model. Next, the LBA model is applied to three sets of data, one from a luminance discrimination task (Ratcliff & Rouder, 1998), and two that used motion discrimination (Mulder, Wagenmakers, Ratcliff, Boekel, & Forstmann, 2012; Van Maanen et al., 2012). To foreshadow, we find that the rise-to-threshold architecture does not always suffice to explain Piéron's Law as present in observed data.

2. Piéron's Law and the LBA model

The LBA model falls into the class of rise-to-threshold evidence accumulation models mentioned earlier. We chose to use the LBA because it is the simplest complete model of choice RT, and thus allows for a clear test of the assumption that empirical Piéron's Law functions can be accounted for by the rise-to-threshold architecture (Brown & Heathcote, 2008). While other choice RT models are simpler (e.g., Carpenter & Williams, 1995; Wagenmakers, van der Maas, & Grasman, 2007), we needed a model that could account for the full suite of fast and slow errors found in the Ratcliff and Rouder (1998) data.

In the LBA, evidence for each potential response is collected in its own accumulator. On each trial, t, evidence for responses is accrued at a linear rate, d_t (and without noise, hence, ballistic) until one accumulator reaches a threshold amount of evidence, b, at which time a decision is made. The activation at the start of each trial, a_t, is a random draw from a uniform distribution with minimum set to zero (without loss of generality) and maximum determined by parameter A. The rate at which evidence accumulates on each trial is a draw from a normal distribution with mean v and standard deviation s. The time taken to make a decision on trial t, therefore, is given by

$$DT_t = (b_i - a_{it})/d_{it}$$

where i indicates the accumulator first to reach threshold. The observed response time for that trial is then

$$RT_t = DT_t + T_{er}$$

where T_{er} is a constant representing the time taken for non-decision aspects of response time, such as stimulus encoding and motor execution.

Evidence for a response accumulates quickly when the stimulus provides a lot of evidence for that response. For example, in a detection task, evidence accumulates quickly for the "stimulus present" response when the stimulus is very intense. Decreasing the intensity of a stimulus, however, will lead to a decrease in the average accumulation rate, $v_{present}$. Since the decision time is inversely proportional to accumulation rate, responses will slow down as accumulation rate decreases.

Fig. 1 displays examples of two LBA accumulators, and provides intuition for why rise-to-threshold accumulator models yield Piéron's law. In the figure, the values of a and b have been arbitrarily set at 0 and 1, respectively, to simplify the demonstration. In the LBA accumulator on the left of Fig. 1, the accumulation rates for the two example trials are relatively fast. In the first accumulator, the rate of accumulation, d_1, is 1, and this yields a decision time of $(1-0)/1 = 1$ s. The second accumulator, d_2, is 0.2 lower, at 0.8, and has a decision time of $(1-0)/0.8 = 1.25$ s. In this first example, when accumulation rate was fast, a decrease in accumulation rate of 0.2 caused a slowdown of 0.25 s. In the LBA on the right side of Fig. 1, the accumulation rates for the two trials are now relatively slow. The rates for the two accumulators were set at $d_1 = 0.65$ and $d_2 = 0.45$, yielding decision times of 1.54 s and 2.22 s, respectively. Note that even though the decrease in accumulation rate from d_1 to d_2 remains 0.2, decision times are now 0.68 s longer in the slower accumulator.

The full LBA model is more complex than that in Fig. 1, as it allows for trial-to-trial variability in parameters. Thus, we now report the results of a simulation study that shows that the full LBA produces Piéron's Law.

2.1. Simulation study to show that the LBA produces Piéron's Law

One thousand data sets were simulated from the LBA, and we examined the relationship between accumulation rate and mean RT. The simulated data were intended to represent data from an experiment in which there were 20 different levels of stimulus intensity or discriminability. As such, we set the mean accumulation rate in the correct accumulator, v, at 20 equally-spaced values between 0.6 and 2. Mean accumulation rate for the incorrect accumulator was set at one minus the mean rate for the correct accumulator (as is standard, Donkin, Brown, & Heathcote, 2009). The remaining parameters were assumed to be constant across the 20 conditions, and were randomly chosen for each data set from the range of reasonable parameters outlined in Donkin, Brown, Heathcote, and Wagenmakers (2011).

For each simulated data set, we fit a power function to the mean RTs and accumulation rates. For each data set, R^2 was calculated to indicate how well the power function described the relationship between accumulation rate and the simulated mean RTs.

The mean R^2 was 0.996, with a standard deviation of 0.002, confirming that the LBA does indeed produce a power-law decrease in mean RT as accumulation rates increase linearly. Since Piéron's Law was originally observed in simple detection tasks, we repeated the simulations assuming just one accumulator. The results are very

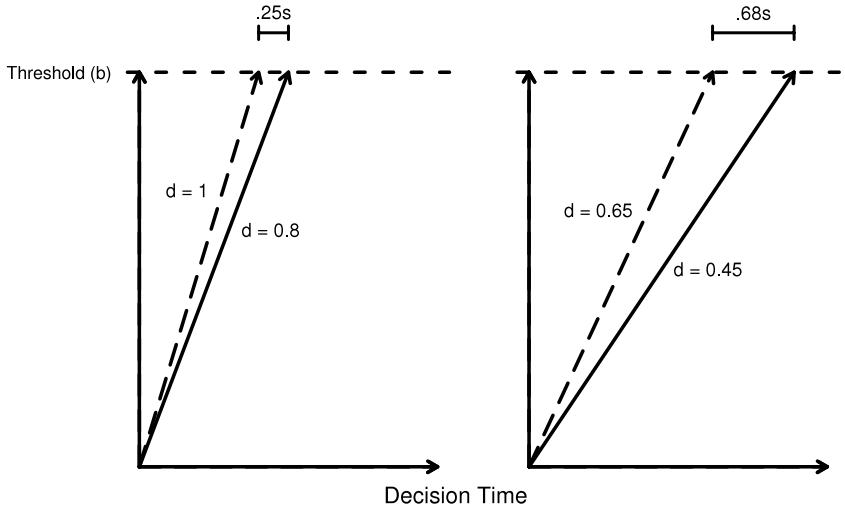

Fig. 1. Example of how Piéron's Law arises out of a rise-to-threshold model, such as the LBA.

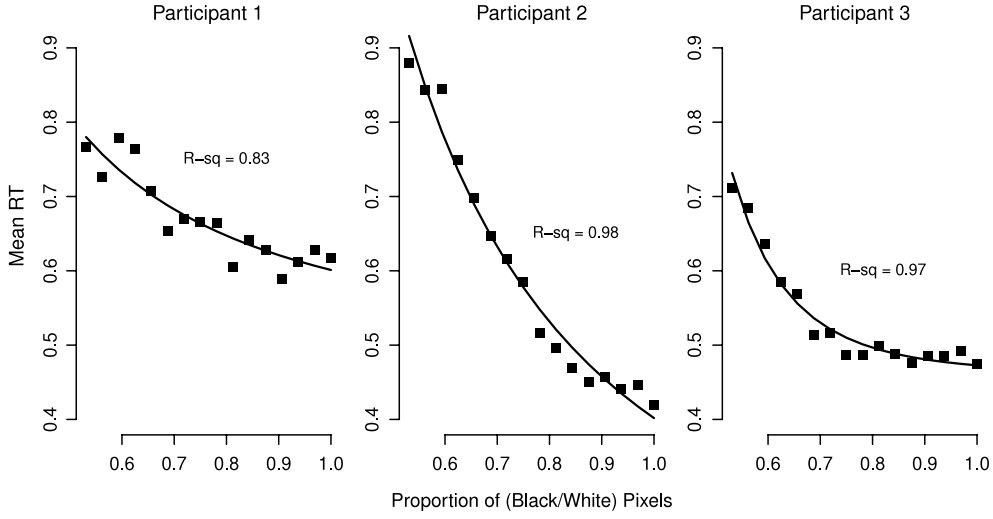

Fig. 2. Mean RT for correct responses as a function of the proportion of white or black pixels in the display. The data are taken from Ratcliff and Rouder (1998). Solid lines are the best fitting power function.

similar, with an average R^2 of 0.992 and a standard deviation of 0.04. Thus, in principle the LBA model can account for Piéron's Law-like behavioral patterns based on a linear relation between accumulation rate and stimulus intensity or discriminability. However, the question remains whether this finding is supported by fits to data that exhibit Piéron's Law.

3. Model application to data

For each of the following three data sets, we will assess the inherent ability of the LBA model's architecture to account for data that shows Piéron's Law. To do so, we will fit a model that assumes a linear relationship between stimulus strength and accumulation rate. If Piéron's Law is entirely the result of the rise-to-threshold architecture of the decision-making process, then this LBA model should be able to fit these data.

3.1. Ratcliff and Rouder (1998)

The first set of data we fit was from Experiment 1 in Ratcliff and Rouder (1998). In their experiment, participants had to decide whether a stimulus made up of black and white pixels was "high" or "low" in luminance. There were 33 equally spaced proportions of black and white pixels from 0% to 100% (i.e., from no black pixels to all black pixels). Feedback in the task was probabilistic, such that stimuli made up of more black than white pixels were more often to be labeled "low" in luminance.[1] In all of the analyses that follow, we collapsed over corresponding 'high' and 'low' luminance conditions, excluding the equal black and white pixels condition, leaving 16 luminance conditions.

3.1.1. Piéron's Law

We first verify that the mean RTs in Ratcliff & Rouder's (1998) data follow a power function of luminance (i.e., Piéron's Law). Fig. 2 shows that for all participants, mean RT increases as the proportion of black and white pixels became closer to 50%. The solid line in

[1] Ratcliff and Rouder also manipulated whether the participants were to respond quickly (speed emphasis) or accurately (accuracy emphasis) in alternating blocks of 204 trials. A power-law relationship between proportion of pixels and mean RT was not readily apparent in the speed emphasis condition, and so here we focus on the accuracy emphasis data. It is important to note that we fit the LBA to both emphasis conditions simultaneously, allowing response threshold only to change with emphasis, and the conclusions about the linearity of the accumulation rate is unchanged. In other words, despite not observing Piéron's Law in mean RT, accumulation rate was still strongly non-linear.

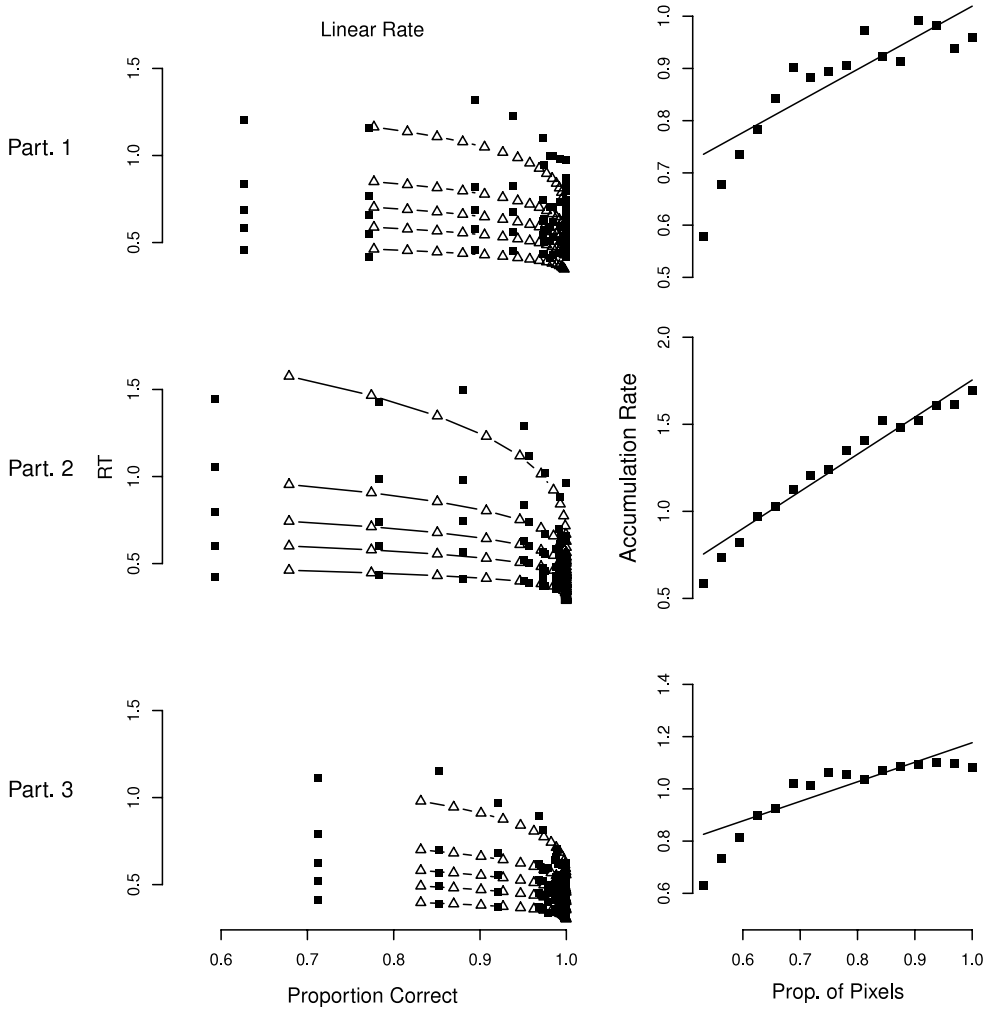

Fig. 3. Model fits and accumulation rates for the Ratcliff and Rouder (1998) data. Left column: Quantile-probability plots showing data (filled squares) and predictions (connected triangles) from the linear rate model. Right column: Accumulation rates estimated from the free rate model plotted as a function of the proportion of black or white pixels. The best-fitting power function through those accumulation rates is represented by the solid line. (Subj = Subject).

Fig. 2 shows the best-fitting power function, which appears to describe well the change in mean RT with stimulus luminance. How well mean RT follows Piéron's Law is also summarized in the figure in the form of R^2.

3.1.2. LBA model fitting

We fit each participant's data with the LBA. In the model, all parameters except accumulation rates were set equal across luminance conditions (i.e., one s, A, b and T_{er} parameter for all 16 conditions). Accumulation rate for the correct response was assumed to follow a linear relationship with luminance, so that

$$v_i = x_0 + x_1 p_i$$

where p_i was the ith proportion of either black or white pixels. Recall that this model will naturally produce Piéron's Law. Accumulation rates for incorrect responses were set at $1 - v_i$. This linear rate LBA model had 6 free parameters.

The likelihood of the model parameters given a chosen response at a particular time is given by Eqs. (1)–(3) in Brown and Heathcote (2008). We used the simplex algorithm with multiple start points to obtain maximum likelihood estimates of the best-fitting parameters for the model, and these are reported in Table 1.

The left column of Fig. 3 plots the fits of the linear rate model in the form of quantile-probability (QP) plots. QP plots are an efficient way of displaying the important information from a set of choice RT data — the horizontal axis contains accuracy information and the vertical axis contains RT distribution information. Each set of horizontally aligned points in the plots represent the RT distributions in a single experimental condition. The horizontal position of a set of points represents the proportion of responses

Table 1
Best-fitting parameter estimates for the linear rate model fit to Ratcliff & Rouder's (1998; RR98), Van Maanen et al.'s (2012; VM12), and Mulder et al.'s (2012; M12) data. Individual participant parameters are shown for the first two data sets, and the minimum, median, and maximum parameters are reported for the Mulder et al. data. For the RR98 data, x_0 and x_1 are in units of proportion of pixels. For VV12, the units are degrees of angular separation. For M12, the units are proportion of dot coherence.

Data set	Participant	s	A	b	T_{er}	x_0	x_1
RR98	1	.25	.34	.62	.16	0.20	0.84
	2	.44	.46	.72	.14	−0.96	3.03
	3	.30	.28	.49	.13	0.07	1.23
VM12	1	.33	.19	.28	.11	0.58	.004
	2	.47	.33	.46	.13	0.80	.003
	3	.29	.48	.76	.10	0.58	0.0007
	4	.26	.33	.60	.23	0.53	0.003
	5	.27	.32	.56	.09	0.53	0.002
	6	.47	.43	.43	.40	0.78	0.008
M12	Minimum	.13	.09	.32	.12	0.47	0.38
	Median	.20	.27	.20	.14	0.52	0.70
	Maximum	.37	.56	.74	.39	0.63	2.15

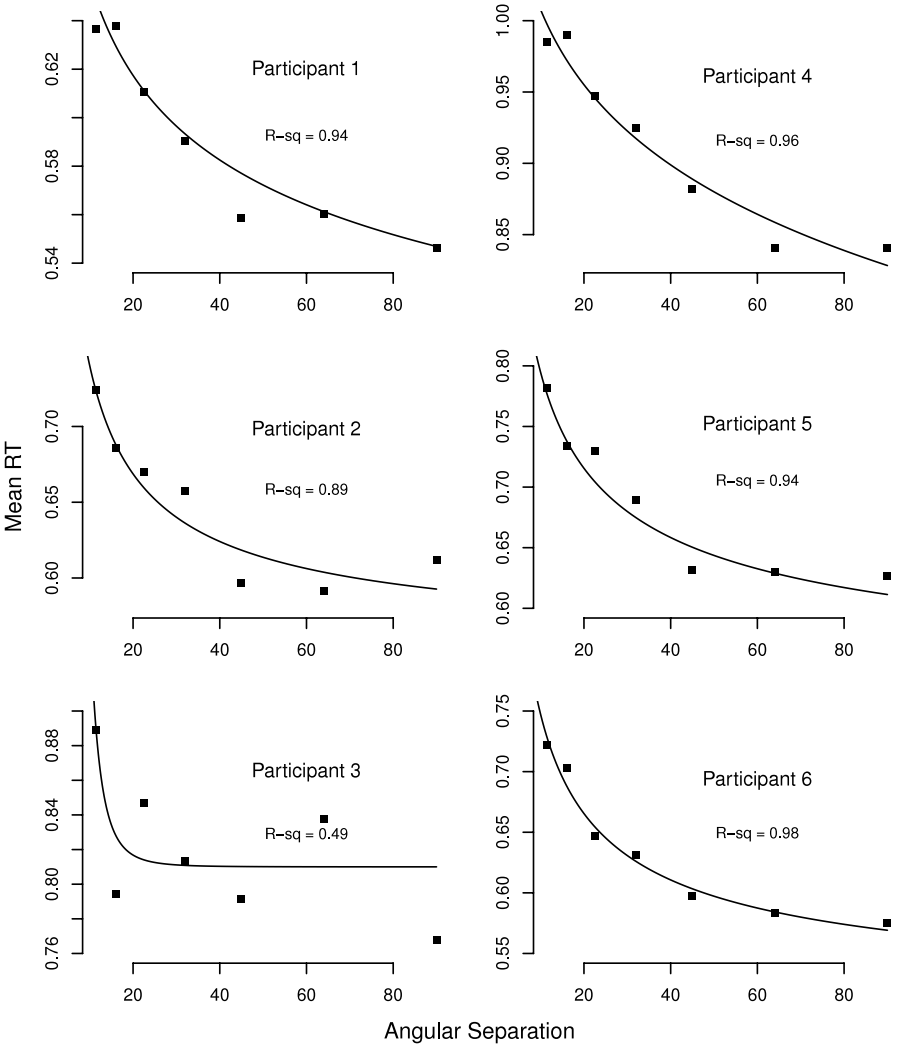

Fig. 4. Mean RT for correct responses as a function of the angular separation between response alternatives in the dot motion task. The data are taken from Van Maanen et al. (2012). Solid lines are the best fitting power function.

making up that RT distribution. As points move to the right of the plot, responses were more accurate, coming from conditions in which the proportion of black or white pixels is closer to 1. The position of points on the vertical axis are determined by the five quantile estimates (.1, .3, .5, .7 and .9). The .1 quantile estimate corresponds to the value below which .1, or 10%, of the RT values in the distribution fall. Therefore, the five quantile values together summarize the RT distribution.

Model predictions in Fig. 3 are represented by the joined open triangles, while the observed RTs are indicated by filled squares. The agreement between the squares and the triangles on both the horizontal and vertical axes reflects the quality of the model's fit. It is clear from the figure that the linear rate model cannot account for the data. The main failure of the model is that it predicts far too high accuracy when the proportion of black or white pixels approached 0.5, as evidenced by the open triangles situated too far to the right of the plot.

As a further test of this hypothesis, we also fit a free accumulation rate model, in which a rate parameter, v_i, is estimated freely for each of the 16 conditions. The free rate model is fit to these data to determine the degree to which accumulation rates are linear when estimated without restriction. The freely estimated accumulation rates are plotted as filled squares in the right column of Fig. 3. It is clear from the figure that the change in rates is non-linear with respect to the proportion of black and white pixels. A best-fitting straight line is drawn through the accumulation rates to highlight this non-linearity.

3.2. *Van Maanen et al. (2012)*

Van Maanen et al. (2012) manipulated the difficulty of a discrimination decision in a random dot motion task. Participants were presented with random dot motion stimuli in which 25% of the dots moved coherently in one of two directions. The participants' task was to indicate the direction in which the dots were moving on that trial. The difficulty of this discrimination was manipulated by changing the angular separation between the two alternative motion directions. Seven different degrees of angular distance were used (11.5°, 16°, 22.5°, 32°, 45°, 64°, and 90°), which varied across trials. Each participant completed 1470 trials, with 210 trials in each angular distance condition providing enough data to fit full RT distributions.

3.2.1. *Piéron's Law*

Van Maanen et al. (2012) showed that a power function provides a good account of the change in mean RT with angular separation between response alternatives. Fig. 4 plots their mean RT data, and shows the best-fitting power function. Piéron's Law is apparent for all but Participant 3.

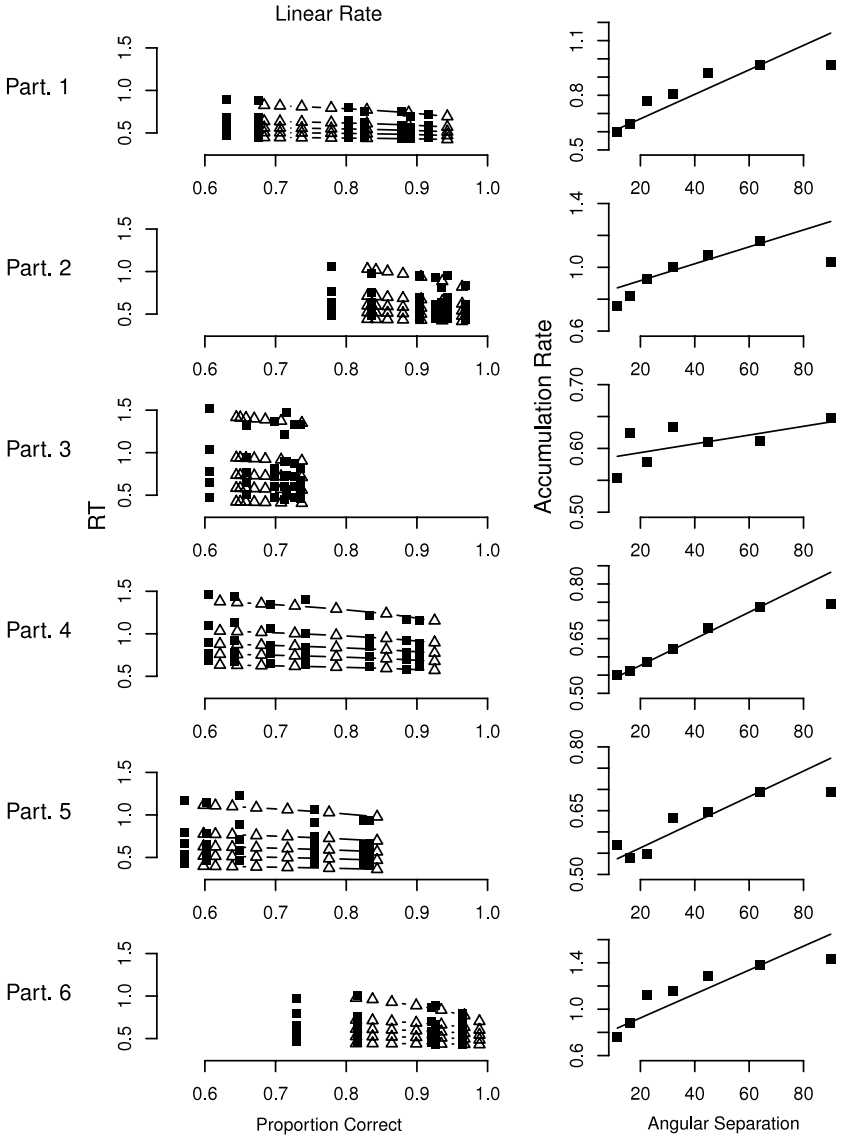

Fig. 5. Model fits and accumulation rates for the Van Maanen et al. (2012) data set. The format of the figure is the same as in Fig. 3.

3.2.2. LBA model fitting

We fit each individual participant with the linear rate LBA model. For the Van Maanen et al. (2012) data, angular separation was manipulated, and all parameters except accumulation rate were fixed as constant across those conditions. The parameterization of the accumulation rates for correct and incorrect responses was exactly the same as for the Ratcliff and Rouder (1998) data set, but now p_i represents the angular distance between response alternatives, in degrees. The best-fitting parameters for each individual are shown in Table 1.

The left panel of Fig. 5 shows the fit of the linear rate model for each participant. These plots are of the same format as Fig. 3. The linear model is unable to account for the full distribution of choice and response times for Participants 1, 2, and 6. However, the fit to Participants 3, 4, and 5 is more reasonable (though recall that Participant 3 does not show Piéron's Law). In general, the fit of the linear rate model is better than it was for the Ratcliff and Rouder (1998) data.

We also fit an LBA model in which the accumulation rates were estimated separately for each level of angular separation. We plotted these accumulation rates in the right panel of Fig. 5. Consistent with the quality of the fits of the linear model, a straight line provides a poor approximation of the estimated accumulation rates for Participants 1, 2, and 6, but it is better for the remaining participants.

3.3. Mulder et al. (2012)

Mulder et al. (2012) had 24 participants perform a random-dot motion task. Unlike the Van Maanen et al. (2012) version of the task, difficulty was manipulated by varying the proportion of dots moving in the same direction. The dot motion coherence was manipulated across the levels 0, 10, 20, 40 and 80 percent, and participants completed 40 trials at each level. The angular separation in this task was held constant at 180°.

3.3.1. Piéron's Law

Fig. 6 plots the mean RT for correct responses as a function of dot motion coherence for each participant. The best fitting power-law function is shown by solid curves. Note that relative to Figs. 2 and 4, the relationship between mean RT and stimulus strength (motion coherence) for the Mulder et al. (2012) data appears to be generally less well fit by a power-law function.

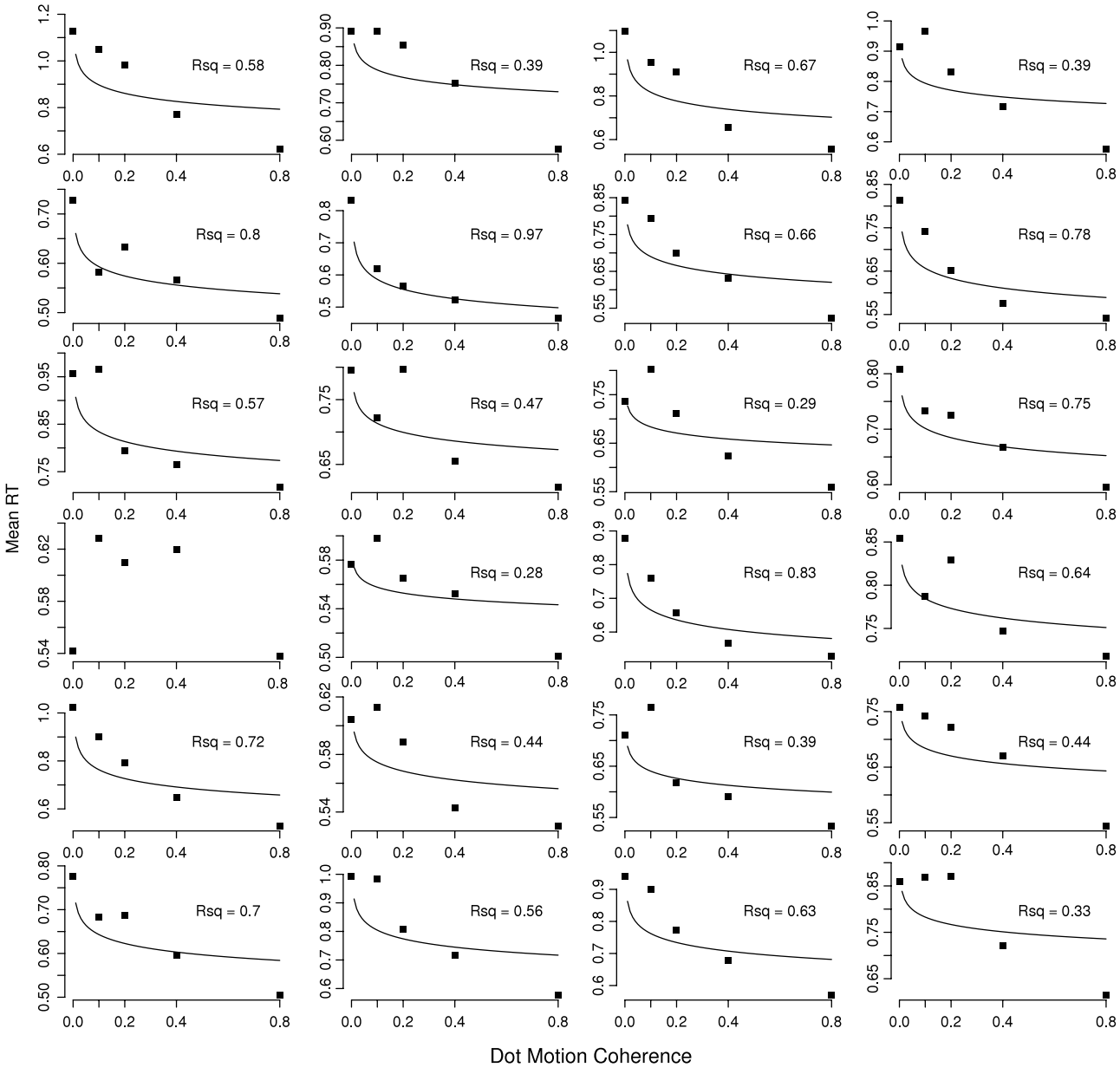

Fig. 6. Mean RT for correct responses as a function of the dot motion coherence. The data are taken from Mulder et al. (2012). Solid lines are the best fitting power function. Note that no good-fitting power function could be found for Participant 4.

3.3.2. LBA model fitting

We again fit the linear rate LBA model to each individual's data. Accumulation rates were assumed to be a linear function of dot motion coherence. All other parameters were held constant across coherence conditions. Rather than report the best-fitting parameter values for each of the 24 individuals, Table 1 contains the minimum, median, and maximum values across those participants.

Fig. 7 shows the fit of the linear rate model to each individual in the Mulder et al. (2012) data set. The linear rate model seems to provide a much better account of these data than it did to the previous two data sets. To seek further evidence for the adequacy of the linear rate model, we plot the freely estimated accumulation rates for each individual in Fig. 8. The solid lines in the figure represent the best-fitting straight lines through those accumulation rates. Unlike the two previous data sets, the accumulation rates in the Mulder et al. (2012) experiment are approximately linear for the majority of participants.

4. General discussion

Stafford and Gurney (2004) showed that Piéron's Law emerges out of a rise-to-threshold decision-making process. Their demonstration implies that Piéron's Law may not reflect anything about the underlying scaling properties of objective stimulus magnitudes. We provided a rigorous empirical test of this claim, assessing the ability of a linear rate model to account for empirical data. In this model, only the architecture of the decision making process could produce Piéron's Law.

4.1. Sometimes Piéron's Law is not just an artifact of the decision-making process

We found that in two data sets in which Piéron's Law was observed, the linear rate model was unable to account for empirical RT distributions and choice probabilities. As such, we conclude that Piéron's Law is not always simply the result of the rise-to-threshold

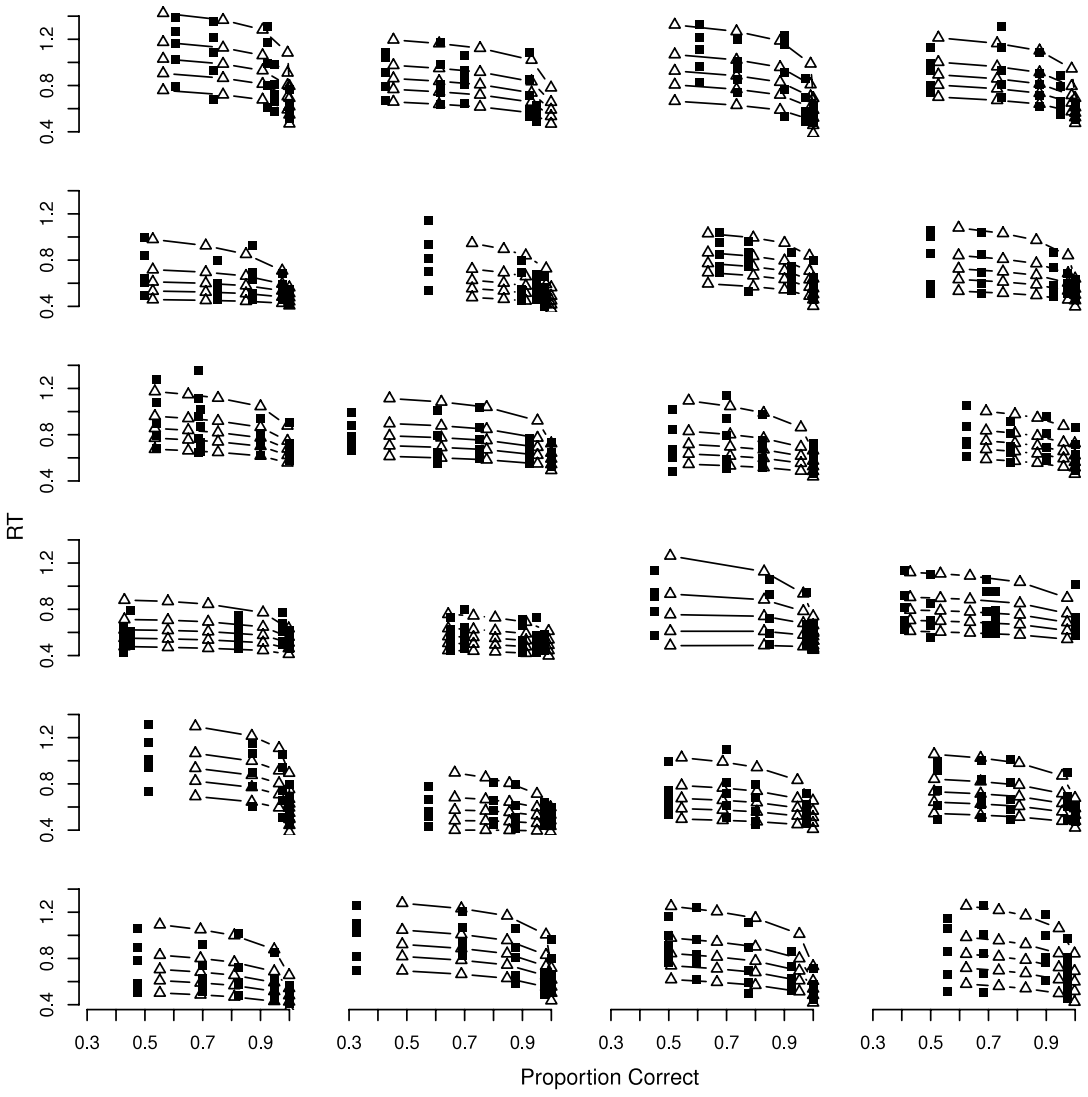

Fig. 7. Fits of the linear rate model to the Mulder et al. (2012) data set. The figure of these quantile-probability plots are the same as in the right column of Figs. 3 and 5.

architecture of the decision-making process. Instead, our results suggest that Piéron's Law is sometimes reflective of a non-linear relationship between the evidence extracted from a stimulus and the strength of that stimulus. In other words, Piéron's Law sometimes reflects a non-linear scaling between objective and subjective representations of stimuli.

Much of the existing literature on Piéron's Law has assumed that Piéron's Law reflects an effect of changing stimulus strength on the processes underlying perception (e.g., Felipe, Buades, & Artigas, 1993; Murray & Plainis, 2003). Our evidence that Piéron's Law is not simply due to the rise-to-threshold of the decision-making mechanism fits well into this literature. Our results are also consistent with those from Carpenter, Reddi, and Anderson (2009), who showed that freely estimated accumulation rates in the LATER model (Carpenter & Williams, 1995) were non-linearly related to contrast (see also Carpenter, 2004; Taylor, Carpenter, & Anderson, 2006).

4.2. Sometimes Piérons Law is just an artifact of the decision-making process

Interestingly, we found that the linear rate model provided a good fit to most participants in a third data set. These data are consistent with Stafford and Gurney's 2004 suggestion that Piéron's Law is a result of the rise-to-threshold architecture of the decision-making process. These results are also consistent with those of Palmer et al. (2005), who also analyzed the relationship between stimulus strength, response time, and accuracy using an evidence-accumulation model. As in Mulder et al. (2012), Palmer et al. used the random dot motion paradigm, and their resultant mean RTs closely followed Piéron's Law. Palmer et al. fit the mean RT and proportion correct data from this experiment with a simple version of a diffusion model (Stone, 1960). They also found that a linear rate model was capable of simultaneously fitting both mean RT and proportion correct, consistent with the claims of Stafford and colleagues (Stafford & Gurney, 2004; Stafford et al., 2011), and Van Maanen et al. (2012).

Thus we observe situations in which Piéron's Law is and is not due to only the decision-making architecture. This result highlights the importance of model fitting when determining whether Piéron's Law reflects the scaling properties underlying the perception of stimuli. We can see no clear reason for the difference in conclusions across experiments, except that perhaps Piéron's Law is weaker in the Mulder et al. (2012) data set. Future work consisting of a series of careful studies is needed to progress our understanding of these differences.

4.3. Identifiability, evidence accumulation, and stimulus scaling

A fundamental assumption in our linear rate model is that the unit of evidence being accumulated in the decision-making model

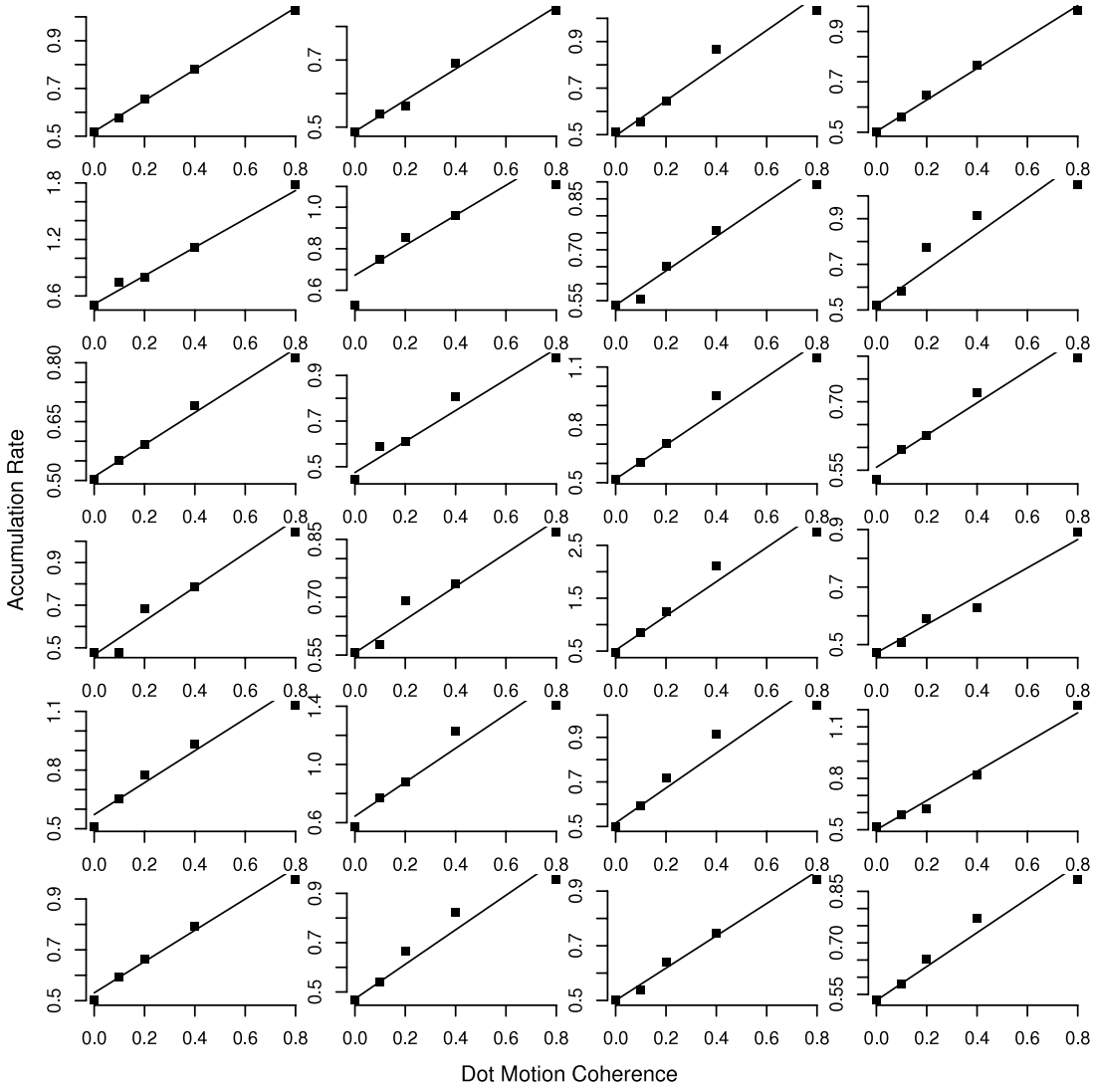

Fig. 8. Freely estimated accumulation rates are plotted as a function of coherence for each individual from the Mulder et al. (2012) data set. The best-fitting linear function is drawn through each set of rates.

is stimulus strength (or linearly related to stimulus strength). Without this assumption, it is impossible to draw any conclusions about stimulus scaling from Piéron's Law. In fact, the assumption of a linear mapping between stimulus strength and the unit of evidence accumulation is also crucial to the claims of Stafford and Gurney (2004) and Van Maanen et al. (2012).

To see this, consider the Ratcliff and Rouder (1998) experiment. We observe a power-law relationship between the proportion of black or white pixels, p, and mean RT (Piéron's Law). The claim we test here is that this power-law relationship arises from the decision-making process. If this claim is true, we should be able to take an RT model, assume a linear mapping between p and accumulation rate, and reproduce Piéron's Law. For the sake of the example, assume that we were able to successfully account for the observed Piéron's Law data with a linear mapping between p and accumulation rate.

Now consider the case where the evidence accumulated is not, in truth, linearly related to p. For example, from an information theory perspective, it may be more sensible to assume that the evidence accumulated is not p, but $\log(\frac{p}{1-p})$. If we fit a model where the unit of evidence accumulation is $\log(\frac{p}{1-p})$, and this is mapped linearly onto accumulation rate, then the model will no longer yield a power-law relationship between mean RT and p. A serious issue of identifiability arises, however, when we consider that there exists an inverse transformation that we could use to map $\log(\frac{p}{1-p})$ to accumulation rate so that the model will again yield Piéron's Law. Such an inverse transformation will exist for the vast majority of assumptions we make about the unit of evidence accumulation.

Let us return to the implications of this issue of identifiability on the claims of Stafford and Gurney (2004) and Van Maanen et al. (2012). If we drop the assumption that the unit of evidence being accumulated is p, then it becomes irrelevant as to whether the decision-making process yields a power-law mean RT function, as there exists an infinite number of transformations between the unit of evidence accumulation and accumulation rate that could yield a linear mapping between p and accumulation rate. As such, if we drop the assumption that the unit of evidence accumulation is p, then Piéron's Law essentially tells us nothing about the perception of p.

4.4. Final comments

In an Appendix, we show that our claims about how well the linear rate model fits data are supported by rudimentary model selection methods. We compared the linear rate model to a non-linear rate model, which assumed a power-law relationship

Table A.1
ΔBIC and BIC weights for the free, linear, power and exponential rate models fit to Ratcliff & Rouder's (1998; RR98) and Van Maanen et al.'s (2012; VM12) data.

Experiment		Model	Participant 1	2	3	4	5	6
RR98	ΔBIC	Linear	108	25	134			
		Non-Linear	0	0	0			
	w	Linear	0	0	0			
		Non-Linear	1	1	1			
VM12	ΔBIC	Linear	22	24	0	0	0	19
		Non-Linear	0	0	5	5	6	0
	w	Linear	0	0	0.94	0.94	0.95	0
		Non-Linear	1	1	0.06	0.06	0.05	1

between stimulus strength and accumulation rate. For the Ratcliff and Rouder (1998) and Van Maanen et al. (2012) data sets, BIC supports the non-linear rate model over the linear rate model. In contrast, the majority of participants in the Mulder et al. (2012) data were preferred by the linear rate model. Since we do not want our conclusions to rest on model selection methods that fail to take into account functional form complexity (Myung & Pitt, 1997), the details of this analysis are presented in an Appendix.

In our linear rate models, stimulus strength had a selective influence on correct accumulation rates. Mean incorrect accumulation rates were assumed to be one minus the mean correct accumulation rate. In accumulator models, one can relax this assumption (Donkin et al., 2009). In an alternative linear rate model, we could instead assume that incorrect accumulation rates followed a separate linear function. We fit this alternative model, and found that the non-linear rate model provided a better account for the data from Ratcliff and Rouder (1998) and Van Maanen et al. (2012). In yet another alternative model, we dropped the assumption of selective influence of stimulus strength of accumulation rate, allowing response thresholds to also vary with stimulus strength (cf. Cavanagh et al., 2011, King, Donkin, Korb, & Egner, 2012). Again, this model provided a less parsimonious account of the data from Ratcliff and Rouder (1998) and Van Maanen et al. (2012) than did the non-linear rate model.

Finally, one might wonder whether the conclusions we draw here are specific to the particular choice response time model we chose to use — the LBA. For example, would the same conclusions be drawn if we had used the popular diffusion model (Ratcliff & Tuerlinckx, 2002). Donkin et al. (2011) found that the parameters of the diffusion and LBA models mapped closely onto one another, and that this was especially the case for the drift rate parameter (see also Winkel et al., 2012). As such, we expect that the same analysis using the diffusion model would yield the same conclusions as we have reached.

Acknowledgment

Chris Donkin's contribution to this research was supported by the Australian Research Council (DP130100124; DE130100129). We also wish to acknowledge Tom Stafford and John Palmer for their extremely helpful comments on earlier versions of this manuscript. Finally, we thank Martijn Mulder for providing the data from Mulder et al. (2012).

Appendix A. Model selection via BIC weights

In order to test the linearity of the accumulation rates, we also fit a non-linear accumulation rate model to each of the three data sets reported in-text. In this non-linear model we assumed that the accumulation rates were a power function of stimulus strength. In particular, we assumed that the accumulation rate for the correct response, v, was related to stimulus strength p by

$$v = x_0 + x_1 p_i^{x_2}.$$

The model was otherwise identical to the linear rate model. Also note that the linear model is nested within the power-law model.

We used Bayesian Information Criterion (BIC) weights (Wagenmakers & Farrell, 2004) to compare the linear and non-linear models. BIC was calculated using

$$\text{BIC} = k \times \log(N) - 2l$$

where l is the likelihood of the parameters given the data, k is the number of free parameters in the model, and N is the number of data points fit by the model. BIC is composed of two terms, $-2l$, which becomes smaller as the agreement between model and data improves, and $k \times log(N)$, which is a penalty term added to the model as it becomes more complex. As such, the model with the smallest BIC gives the most parsimonious account of the data.

To aid interpretation, we transform BIC values into BIC weights. The BIC weight represents the probability that model i is the true data-generating model, assuming that one of the fitted models is the true model. The BIC weight for the ith model, w_i is calculated using

$$w_i(\text{BIC}) = \frac{e^{-\frac{1}{2}\Delta_i \text{BIC}}}{\sum_k e^{-\frac{1}{2}\Delta_k \text{BIC}}}$$

where Δ_iBIC is the difference between the smallest BIC value (for each participant) and the BIC of the ith model.

Table A.1 contains ΔBIC and BIC weights for the linear and non-linear rate models for each participant in the Ratcliff and Rouder (1998) and Van Maanen et al. (2012) data sets. For the Ratcliff and Rouder (1998) data, all three participants were fit better by the non-linear model than the linear model. BIC weights for the three participants were 0 for the linear rate model. The linear rate model found more support in the Van Maanen et al. (2012) data. The linear rate model best fit the data from 3 of the 6 participants.

The Mulder et al. (2012) data yields stronger support for the linear rate model. Twenty out of the 24 participants were better fit by the linear rate model than the non-linear rate model. The BIC weight, averaged over participants, for the linear rate model was 0.75, suggesting that the linear rate model was almost three times as likely to have generated the data from Mulder et al. (2012) than the non-linear rate model.

One may wonder about the overall quality of the fits of the linear and non-linear models. We can assess this by comparing the log-likelihood fits of the linear and non-linear models to the model in which rate parameters are freely estimated across stimulus strength conditions. The free rate model is almost a saturated model, and thus provides a benchmark against which we can compare the fits of the much simpler linear or non-linear models. For the Ratcliff and Rouder (1998) data, the log-likelihood values of the free-rate models were −5185, −4438, and −4205 for the three participants, respectively. The log-likelihoods for the linear model are −5246, −4461, and −4282. The log-likelihoods for the

non-linear model are −5187, −4442, and −4209. Note that the non-linear model, despite having 13 fewer free parameters, fits the data almost as well as the free rate model. The log-likelihood values for the Van Maanen et al. (2012) participants are −3592, −3388, −2987, −3660, −3833, −3328 for the free rate model; are −3611, −3408, −2991, −3665, −3841, −3347 for the linear rate model; and −3596, −3393, −2990, −3664, −3840, and −3334 for the non-linear model. For the Mulder et al. (2012) data set, for 12 of the 24 participants, the linear rate model was within 2 log-likelihood points of the free rate model, and 8 participants were within 2 and 4 points. The non-linear rate model was within 2 log-likelihood points of the free rate model for 19 of the 24 participants, and within 4 points for the remaining participants.

References

Aguirre, R. C., Colombo, E. M., & Barraza, J. F. (2008). Effect of glare on simple reaction time. *Journal of the Optical Society of America A*, *25*, 1790–1798.

Bonnet, C., Zamora, M. C., Buratti, F., & Guirao, M. (1999). Group and individual gustatory reaction times and pieron's law. *Physiology & Behavior*, *66*, 549–558.

Brown, S. D., & Heathcote, A. J. (2008). The simplest complete model of choice reaction time: Linear ballistic accumulation. *Cognitive Psychology*, *57*, 153–178.

Burr, D. C., Fiorentini, A., & Morrone, C. (1998). Reaction time to motion onset of luminance and chromatic gratings is determined by perceived speed. *Vision Research*, *38*, 3681–3690.

Carpenter, R. H. S. (2004). Contrast, probability, and saccadic latency: Evidence for independence of detection and decision. *Current Biology*, *14*, 1576–1580.

Carpenter, R. H. S., Reddi, B. A. J., & Anderson, A. J. (2009). A simple two-stage model predicts response time distributions. *Journal of Physiology*, *587*, 4051–4062.

Carpenter, R. H. S., & Williams, M. L. L. (1995). Neural computation of log likelihood in control of saccadic eye movements. *Nature*, *377*, 59–62.

Cavanagh, J. F., Wiecki, T. V., Cohen, M. X., Figueroa, C. M., Samnta, J., Sherman, S. J., et al. (2011). Subthalamic nucleus stimulation reverses mediofrontal inuence over decision threshold. *Nature Neuroscience*, *14*, 1462–1467.

Donkin, C., Brown, S. D., & Heathcote, A. (2009). The over-constraint of response time models: Rethinking the scaling problem. *Psychonomic Bulletin & Review*, *16*, 1129–1135.

Donkin, C., Brown, S., Heathcote, A. J., & Wagenmakers, E.-J. (2011). Diffusion versus linear ballistic accumulation: Different models for response time, same conclusions about psychological mechanisms?. *Psychonomic Bulletin Review*, *55*, 140–151.

Felipe, A., Buades, M. J., & Artigas, J. M. (1993). Influence of the contrast sensitivity function on the reaction time. *Vision Research*, *33*, 2461–2466.

King, J. A., Donkin, C., Korb, F. M., & Egner, T. (2012). Model-based analysis of context-specific cognitive control. *Frontiers in Psychology*, *3*, 358.

Luce, R. D. (1986). *Response times*. New York: Oxford University Press.

Mulder, M. J., Wagenmakers, E.-J., Ratcliff, R., Boekel, W., & Forstmann, B. U. (2012). Bias in the brain: A diffusion model analysis of prior probability and potential payoff. *Journal of Neuroscience*, *32*, 2335–2343.

Murray, I. J., & Plainis, S. (2003). Contrast coding and magno/parvo segregation revealed in reaction time studies. *Vision Research*, *43*, 2707–2719.

Myung, I. J., & Pitt, M. A. (1997). Applying Occam's razor in modeling cognition: A Bayesian approach. *Psychonomic Bulletin & Review*, *4*, 79–95.

Nachmias, J., & Kocher, E. C. (1970). Visual detection and discrimination of luminance increments. *Journal of the Optical Society of America A*, *60*, 382–389.

Overbosch, P., de Wijk, R., de Jonge, T. J., & Koester, E. P. (1989). Temporal integration and reaction times in human smell. *Physiology & Behavior*, *45*, 615–626.

Palmer, J., Huk, A. C., & Shadlen, M. N. (2005). The effect of stimulus strength on the speed and accuracy of a perceptual decision. *Journal of Vision*, *5*, 376–404.

Piéron, H. (1914). Recherches sur les lois de variation des temps de latence sensorielle en fonction des intensit's excitatrices. *L'Annee Psychologique*, *20*, 17–96.

Piéron, H. (1952). *The sensations: Their functions, processes, and mechanisms*. London: Mueller.

Pins, D., & Bonnet, C. (1996). On the relationship between stimulus intensity and processing time: Piéron's law and choice reaction time. *Perception & Psychophysics*, *58*, 390–400.

Ratcliff, R. (1978). A theory of memory retrieval. *Psychological Review*, *85*, 59–108.

Ratcliff, R., & Rouder, J. N. (1998). Modeling response times for two–choice decisions. *Psychological Science*, *9*, 347–356.

Ratcliff, R., & Tuerlinckx, F. (2002). Estimating parameters of the diffusion model: Approaches to dealing with contaminant reaction times and parameter variability. *Psychonomic Bulletin & Review*, *9*, 438–481.

Reddi, B. A. J., Asrress, K. N., & Carpenter, R. H. S. (2003). Accuracy, information, and response time in a saccadic decision task. *Journal of Neurophysiology*, *90*, 3538–3546.

Servant, M., Montagnini, A., & Burle, B. (2014). Conflict tasks and the diffusion framework: Insight in model constraints based on psychological laws. *Cognitive Psychology*, *72*, 162–195.

Stafford, T., & Gurney, K. (2004). The role of response mechanisms in determining reaction time performance: Piéron's law revisited. *Psychonomic Bulletin & Review*, *11*, 975–987.

Stafford, T., Ingram, L., & Gurney, K. N. (2011). Piéron's law holds during Stroop conflict: insights into the architecture of decision making. *Cognitive Science*, *35*, 1553–1566.

Stone, M. (1960). Models for choice–reaction time. *Psychometrika*, *25*, 251–260.

Taylor, R. H. S., Carpenter, R. H. S., & Anderson, A. J. (2006). A noisy transform predicts saccadic and manual reaction times to changes in contrast. *Journal of Physiology*, *573*, 741–751.

Van Maanen, L., Grasman, R. P. P. P., Forstmann, B. U., & Wagenmakers, E.-J. (2012). Piéron's law and optimal behavior in perceptual decision making. *Frontiers in Decision Neuroscience*, *5*, 143.

Wagenmakers, E.-J., & Farrell, S. (2004). AIC model selection using Akaike weights. *Psychonomic Bulletin & Review*, *11*, 192–196.

Wagenmakers, E.-J., van der Maas, H. J. L., & Grasman, R. P. P. P. (2007). An EZ-diffusion model for response time and accuracy. *Psychonomic Bulletin & Review*, *14*, 3–22.

Winkel, J., Van Maanen, L., Ratcliff, R., Van Der Schaaf, M. E., Van Schouwenburg, M. R., Cools, R., & Forstmann, B. U. (2012). Bromocriptine does not alter speed-accuracy tradeoff. *Frontiers in Decision Neuroscience*, *6*, 126.